Kinetics and Catalysis, Vol. 41, No. 2, 2000, pp. 222–230. Translated from Kinetika i Kataliz, Vol. 41, No. 2, 2000, pp. 245–254.

Oxidative Ammonolysis of Methylpyrazine over Binary Catalytic Systems: III. Phosphorus–Molybdenum System: Catalytic Properties and the Active Component

V. M. Bondareva, T. V. Andrushkevich, N. N. Chumachenko, R. I. Maksimovskaya, L. M. Plyasova, V. V. Malakhov, L. S. Dovlitova, E. B. Burgina, and G. S. Litvak

Boreskov Institute of Catalysis, Siberian Division, Russian Academy of Sciences, Novosibirsk, 630090 Russia

Received May 5, 1998

Abstract—The phase composition of the binary phosphorus–molybdenum system with a Mo/P ratio of 3–24.5 and its catalytic properties in the reaction of oxidative ammonolysis of methylpyrazine are studied. X-ray amorphous phases of molybdenyl phosphate and phosphorus modified molybdenum trioxide are active in the formation of pyrazinonitrilee.

INTRODUCTION

Analysis of patents [1–3] and literature data [4–6] shows that, in addition to vanadium-containing compositions, catalysts based on molybdenum oxide (including phosphorus–molybdenum catalysts) can be used in the reactions of the oxidative ammonolysis of methylpyrazine.

The formation of discrete heteropoly anions (HPAn) with various compositions (Mo/P = 5/2–12/1) [7] is typical of the binary Mo(VI)–P(V) system with a high molybdenum content. Molybdenum phosphates (Mo/P = 1/1 and 1/2) [8] are formed at a higher phosphorus concentration. Heteropoly acids (HPAc) of the 12th row (Mo/P = 12) are studied better than others. Their structures, thermolysis, as well as acid–base, redox, and catalytic properties were studied. It is known that the main disadvantage of HPAc-based catalysts is their relatively low stability at high temperatures and in the reductive reaction medium. The study of HPAc behavior in the reaction of acrolein oxidation [9] showed that the products of HPAc thermolysis, such as its anhydride ($PMo_{12}O_{38.5}$) and molybdenyl phosphates ($(MoO_2)_2P_2O_7$ and $(MoO_2)HPO_4$), exhibit maximal selectivity.

The study of the catalytic properties of PMo–HPAc in the reaction of the oxidative ammonolysis of methylpyrazine [10] showed that, at 360–380°C, the maximal yield of pyrazine nitrile is equal to 60–65%. In the reaction mixture containing a large amount of ammonia, HPAc converts into the respective ammonium salt (HPS).

The data on catalytic and physicochemical properties of phosphorus–molybdenum system are scarce. In [11], the activity of samples with the ratios P/Mo = 1/1 and 1/12 in the reaction of ammonia oxidation was measured. The catalytic properties of the system in the oxidation reaction of butenes and their derivatives into furan and in the reaction of acrolein oxidation into acrylic acid were characterized in [12–14] and [15], respectively. When going from pure phosphorus oxide to pure molybdenum oxide, the maximum activity is at Mo/P = 10–12 [12–15].

The aim of this work was to study the catalytic properties and determine the active component of the phosphorus–molybdenum oxide system in the oxidative ammonolysis of methylpyrazine.

EXPERIMENTAL

Binary phosphorus–molybdenum catalysts with the ratios Mo/P = 4.5, 7.8, 12, and 24.5 were obtained by the evaporation of solutions of ammonium paramolybdate (APM) and orthophosphoric acid (pH of the solution was maintained at ~7) followed by the stepwise thermal treatment of the product at 110°C (6 h), 200°C (3 h), and 400°C (5 h) in air. An increase in the temperature leads to a change in the sample color from white to yellow-green, and then to blue. The sample with the Mo/P = 3 ratio was obtained in an analogous way from the solution of orthophosphoric and molybdenum acids (pH ~ 1). The sample immediately became yellow and, after calcination at 400°C, it became dark blue. When preparing the samples with a higher phosphorus concentration (Mo/P < 3), the glassy substance was formed. This substance melted at a temperature higher than 200°C. These samples were not studied.

Thermal studies were carried out in air using a Q-1500D (Hungary) derivatograph with a heating rate of 10 K/min. We used platinum crucibles. Samples weighed 200 mg.

XRD spectra were measured by a URD-6 (Germany) diffractometer using filtered CuK_α irradiation (a graph-

0023-1584/00/4102-0222$25.00 © 2000 MAIK "Nauka/Interperiodica"

ite monochromator with a reflected beam). XRD measurements were carried out at $2\theta = 5°–70°$ at a record rate of 1 and 0.5 degree/min. Parameters of MoO_3 lattice were determined by the least-squares method using the POLIKRISTALL program [16].

Phase analysis was carried out by the method of differential dissolution using a setup similar to [17]. A portion of a substance was put in a flow microreactor. The flow of the solvent (an aqueous solution of ammonia) passed through a reactor. The ammonia concentration and the temperature increased with time from 0 to 3% and from 2 to 30°C, respectively. The out-flow from the reactor was directed to the detector/analyzer of elemental composition (that is, to the atomic emission spectrometer with induction confined plasma). The setup enabled almost continuous recording of the kinetic curves of the dissolution of elements constituting a catalyst. Data acquisition and data processing were carried out with a computer. The general method of calculations was described in [18].

The IR spectra of samples were measured by a SPECORD IR-75 spectrometer at 200–1500 cm^{-1}. A portion of a sample (2 mg) was pressed into pellets after mixing with 500 mg of KBr.

The MAS ^{31}P NMR spectra of solid samples were measured with a BRUKER CXP-300 spectrometer. The working frequency was equal to 121.47 MHz (spectrum width was 10 and 50 kHz, pulse was equal to 10 μs, the number of repetitions was 20–1000 every 90 s). The ^{31}P NMR spectra of solutions were measured with a BRUKER MSL-400 spectrometer (the frequency was 161.677 MHz in an interval of 10 kHz, the high-frequency pulse was ≤30°, the number of repetitions was 10–100 every 30 s). Distilled water was added to a sample, the suspension was mixed, a solution was poured out, and then the ^{31}P NMR spectrum of the water extract was measured. The Mo/P ratio in the solution was determined by the measurement of the relative content of all phosphorus–molybdenum complexes. This content was calculated from the intensity of NMR ^{31}P signals. The method of water extraction and of the calculation of the Mo/P ratio was described in detail in [19]. Chemical shifts (δ) were determined using the 85% solution of H_3PO_4 as an external reference.

The catalytic properties of samples were studied in a flow setup by the chromatography of the components of reaction mixture. The tests were carried out at 300–380°C. The reaction mixture had the following composition (vol %): $C_5H_6N_2$ 1.5–2.0, O_2 7–8, NH_3 15–17, H_2O 15–17, and nitrogen balance. Methylpyrazine conversion, the selectivity of product formation, and the carbon balance were calculated from the experimental data. The specific rate constants of total methylpyrazine conversion (k_1) calculated using the first-order equation, as well as the maximal yield of pyrazinonitrile (Y_{max}), were used to compare the catalytic properties of samples. Detailed description of the experimental setup, conditions of chromatographic analyses, and calculation of experimental data are given in [20].

RESULTS AND DISCUSSION

DTA and DTG curves for phosphorus–molybdenum catalysts dried at 110°C, as well as for APM and H_3PO_4 used as initial compounds for sample preparation, are presented in Fig. 1.

The character of thermal curves of phosphorus–molybdenum samples differs from those of initial compounds. This is evidence for the interaction of APM and H_3PO_4 leading to the formation of new compounds. The main product of the interaction of phosphorus with molybdenum is the ammonium salt of PMo–HPAc. The XRD spectra of all samples have the set of reflexes (d/n = 8.07, 5.77, 4.74, 4.114, 3.663, 3.346, 3.104, 2.8974, 2.7352, and 2.4747 Å) typical of the HPAc salts of the 12th row with a cubic structure. The ^{31}P NMR spectrum of solid samples is also typical of HPAc and is a unique narrow band with $\delta = -4.4$ ppm. HPS is formed during mixing (in acidic solutions with pH ≤ 1) or during the subsequent thermal treatment at 200°C [15]. The Mo/P ratio in HPS is equal to 12. The excess of molybdenum and phosphorus in binary samples as compared to HPS seems to be present as other compounds, which are not detected by the methods described above.

Figure 1 (curves *1* and *7*) shows that the decomposition of APM and H_3PO_4 with the formation of molybdenum trioxide and polyphosphoric acid is completed at 360°C. Therefore, all effects observed at a higher temperature for binary samples correspond to the transformation of interaction products. The presence of several high-temperature peaks at 410–470°C in DTA curves is evidence for several steps included in the process of HPS thermal decomposition. For example, this could be the formation of intermediate acid salts, HPAc, or its anhydride. The decomposition of HPC is accompanied by the mass loss due to the removal of water and ammonia vapor. The reduction of the salt or the products of its thermolysis is possible during this process. An intensive exothermic peak with a maximum at 500–545°C accompanied by an increase in mass is probably explained by the reoxidation of Mo^{5+} to Mo^{6+}. A stepwise character of the thermolysis of partially reduced HPAc was observed in [22]. This character is due to the nonequivalency of structural protons.

Thermochemical data suggest that the thermal treatment of samples at 400°C for 5 hours can lead to the partial reduction of HPS and to the destruction of the Keggin anion.

XRD spectra of all samples calcined at 400°C are similar and contain only reflexes typical of the rhombic modification of molybdenum trioxide independently of their composition. However, a certain shift of reflexes as compared to MoO_3 was observed in XRD spectra.

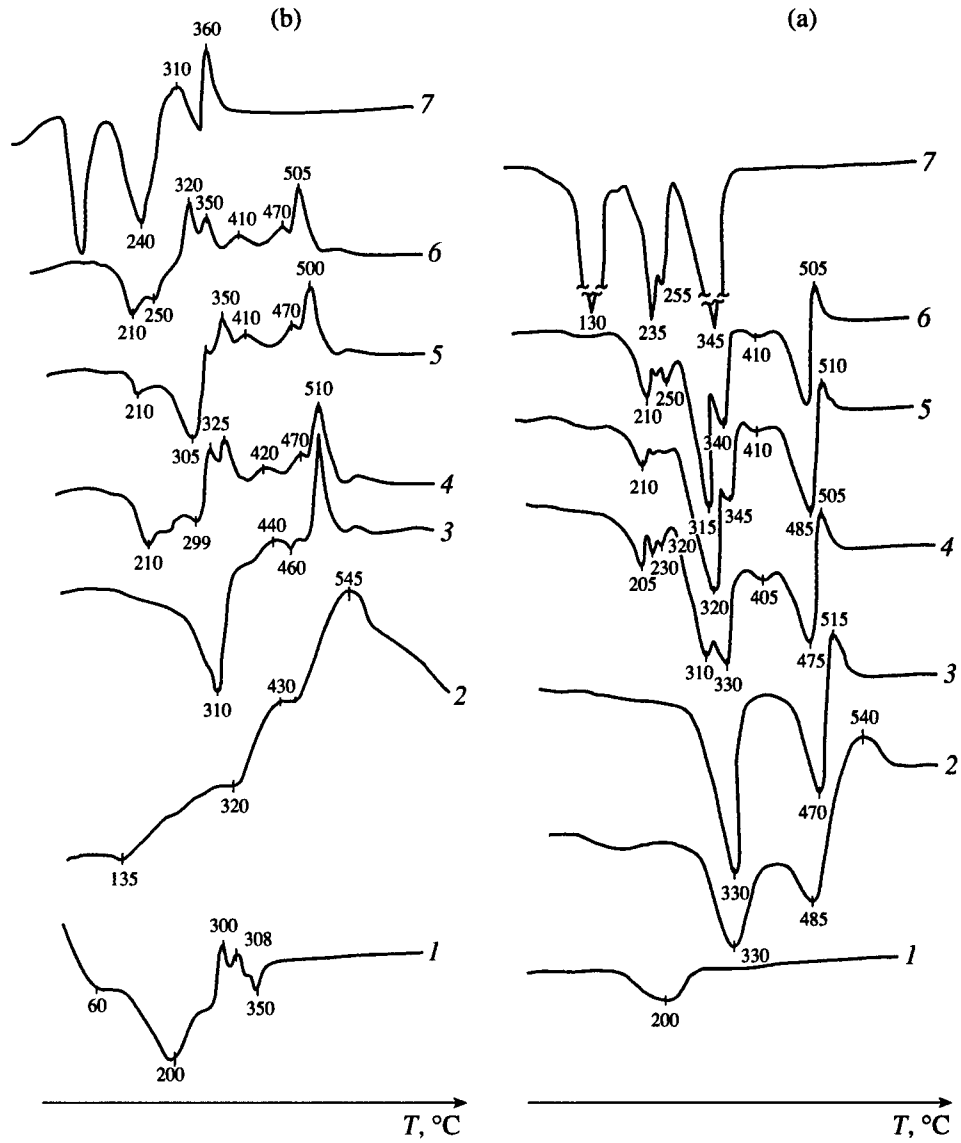

Fig. 1. (a) DTA and (b) DTG curves for (*1*) orthophosphoric acid [21], binary samples with Mo/P = (*2*) 3.0, (*3*) 4.5, (*4*) 7.8, (*5*) 12.0, (*6*) 24.5, and for (*7*) ammonium paramolybdate.

Table 1 presents the parameters of lattice of the samples and, for comparison, the respective data for MoO_3.

The lattice parameters of binary samples are higher than the values tabulated for MoO_3. A change in the parameter *b* is more pronounced. This confirms that phosphorus incorporates into the MoO_3 lattice and changes the layer-to-layer distance (parameter *b*) more than other parameters. Within the accuracy of lattice parameter determination, it is impossible to quantitatively analyze the dependence of parameters *a*, *b*, and *c* on the phosphorus concentration. Nevertheless, there is a certain trend toward increasing the parameter *b* with an increase in the phosphorus amount. The maximal deviation of parameter *b* is typical of the sample with the maximal phosphorus concentration, that is, for the sample with Mo/P = 3. A substantial broadening of XRD signals prevents the precise measurement of lattice parameters.

It is necessary to note that an increase in the phosphorus concentration is accompanied by a decrease in the intensity of MoO_3 reflexes in XRD spectra and by their broadening. This permits us to suppose that the samples contain not only modified oxide but also amorphous phase or phases.

The IR spectra of all calcined samples (Fig. 2) contain absorption bands typical of molybdenum trioxide. [24]. These absorption bands are also somewhat shifted like XRD reflexes. Apparently, this is also due to the introduction of phosphorus to MoO_3. Absorbance at 1000–1200 cm^{-1} corresponds to the stretching of the P–O bond [25]. This is evidence for the existence of phosphate phases in the samples. In addition, the spectra of samples with Mo/P < 7.8 contain an additional absorption band at 1410 cm^{-1} typical of NH_4^+ ions [25]. The intensity of this band, as well as the intensity of the

absorbance at 1000–1200 cm^{-1}, increases with an increase in the phosphorus concentration. Taking into account the composition of the initial compounds, we conclude that all samples contain not only modified molybdenum trioxide but also molybdenum phosphates. The samples with Mo/P < 7.8 contain also ammonium phosphate. According to the literature data [8, 26], molybdenum phosphates (Mo/P = 1/1 and 1/2) and molybdenum polymetaphosphates $(NH_4PO_3)_n$, which are the products of ammonium phosphate dehydration [27], can be X-ray amorphous.

Figure 3a presents the ^{31}P MAS NMR spectrum of the solid sample with Mo/P = 7.8. The parameters of this spectrum (chemical shift and width) are the same for all samples and coincide with earlier spectra of the products of HPAc thermolysis, that is, a mixture of phases of molybdenyl phosphates ($(MoO_2)_2P_2O_7$ and $(MoO_2)HPO_4$) [28]. Spectral bands corresponding to heteropoly compounds were not detected. This can be due to HPAc destruction or their partial reduction in the calcination process leading to a significant broadening of the respective spectral bands. In the ^{31}P NMR spectra of the samples with Mo/P = 3 and 4.5, the bands of polymetaphosphate were not observed either. This is probably due to their significant broadening.

Figure 3b presents the ^{31}P MNR spectra of three subsequent water extracts. All spectra of water extracts consist of several signals. We used the results of [29, 30] for their identification. The ratio Mo/P in the fist extract is close to unity. This fact and the spectrum are evidence for the presence of molybdenyl phosphates. The ratio Mo/P in the next extracts increases to 12. A similar result was observed earlier in the study of the composition of water-soluble products of PMo–HPA thermolysis [28, 29]. However, the set of signals in the spectra of the second and the third extracts is somewhat different. The bands with $\delta = -3.7$ ppm, typical of the heteropoly anion $[PMo_{12}O_{40}]^{3-}$, disappear, and new signals at 0.2 and –6.6 ppm appear. According to [30], these two bands correspond to a HPAn reduced by one and two electrons, respectively. It is obvious that reduction takes place due to the removal of ammonia upon calcination. It is yet unclear which compound contains this heteropoly anion: acid salt, HPAc, or its anhydride. Note only that its amount is not large, and this means that HPS decomposes substantially upon calcination.

The method of differential dissolution permits us to obtain data on the composition (fragment formula without taking into account oxygen) and the quantity of various phases. Figure 4 presents parametric kinetic curves of phosphorus and molybdenum dissolution and stoichiometry (the P/Mo ratio) as functions of the degree of sample dissolution for the sample with Mo/P = 7.8. Similar curves were obtained for the samples with other compositions.

According to the experimental data, all samples contain two forms of molybdenum compounds with phosphorus characterized by a different solubility and

Table 1. Lattice parameters of phosphorus–molybdenum catalyst samples

Composition	*a*	*b*	*c*
MoO_3*	3.9628(6)	13.855(3)	3.6964(7)
Mo/P = 3.0	3.969(9)	14.06(7)	3.698(2)
Mo/P = 4.5	3.971(9)	13.94(5)	3.705(4)
Mo/P = 7.8	3.968(7)	13.96(2)	3.701(2)
Mo/P = 12.0	3.979(7)	13.90(1)	3.700(2)
Mo/P = 24.5	3.974(7)	13.92(1)	3.702(2)

* Data from the JCPDS files [23].

Table 2. Results of analysis of PMo systems by the method of differential dissolution

Mo/P	Content, wt %		x in Mo_1P_x	Content of a phase, wt %		
	form I	form II		P_1Mo_1	P_1Mo_{12}	P_1Mo_x
3.0	65	35	0.054	26.5	3.8	69.7
4.5	56	44	0.042	21.5	4.6	73.9
7.8	15	85	0.036	4.7	0.9	94.4
12.0	12	88	0.023	2.5	0.7	96.8
24.5	7	93	0.015	0.9	0.3	98.8

elemental ratio. The first form (I) is readily soluble in water, whereas the fast solution of the second form (II) takes place as H_2O gradually substitutes NH_4OH. The maximal value of P/Mo in form I is 10–20 times higher than in form II. A change in P/Mo over the part of the stoichiogram (Fig. 4) corresponding to the dissolution of form I and to the beginning of the dissolution of form II is evidence for the absence of the efficient separation of individual phases under the conditions of differential dissolution. However, the part of the stoichiogram corresponding to the dissolution of the main part of form II corresponds to the phase with constant P/Mo = $x < 0.06$. Taking into account the data of XRD and IR measurements, this phase can be considered as modified molybdenum trioxide, the value of x characterizing the degree of MoO_3 modification by phosphorus. When increasing the content of phosphorus in the samples, the part of water-soluble form I and the value of x increase monotonically.

^{31}P NMR measurements show that water-soluble compounds are molybdenyl phosphates (fragment formula is P_1Mo_1) and reduced HPAc or HPS (fragment formula is P_1Mo_{12}). Using these data and the results of differential dissolution on the degree of MoO_3 modification by phosphorus (fragment formula is Mo_1P_x) and using stoichiometric calculations, we can transform the curves of element dissolution into the kinetic curves for the dissolution of individual phases. Figure 5 presents an example of such transformation for the sample with Mo/P = 7.8. It is seen from Fig. 5 that the phase PMo_{12} is distributed between both forms. The presence of PMo_{12} in form II confirms that a part of this phase lies

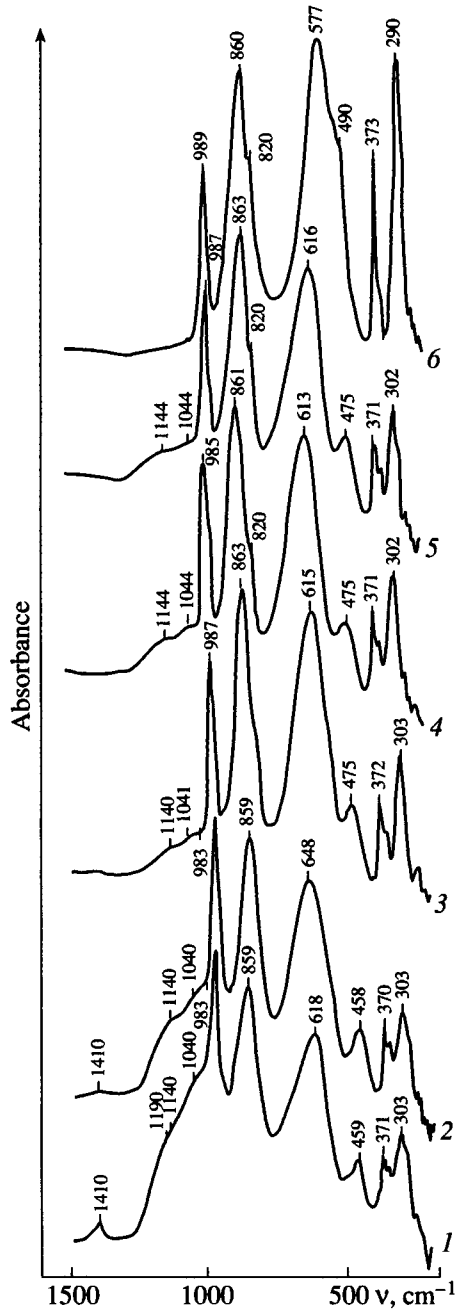

Fig. 2. IR spectra of binary samples with Mo/P = (*1*) 3.0, (*2*) 4.5, (*3*) 7.8, (*4*) 12.0, (*5*) 24.5, and (*6*) of a MoO_3 sample.

in the deep regions of the porous structure in the main phase, which is a modified molybdenum trioxide phase. The samples may also contain a small amount (less than 2 wt %) of the "pure" MoO_3 phase.

Table 2 presents the quantitative data on the phase composition of the samples.

Thus, our study showed that all the samples of the oxide phosphorus–molybdenum system calcined at 400°C are multiphase and in general consist of molybdenyl phosphate and molybdenum trioxide modified by phosphorus. There is also a small amount of the phase of the partially reduced heteropoly compound. The difference between the samples consists only in the different relative content of these phases. In addition, in the samples with Mo/P < 7.8, there is a phase of ammonium polymetaphosphate. The sample with the maximal content of phosphorus (Mo/P = 3) contains the maximal quantity of this phase.

Further reduction of heteropoly anions and HPS destruction takes place in the oxidative ammonolysis of methylpyrazine. This conclusion can be drawn from the disappearance of heteropoly anion signals from the spectra of water extracts of the samples treated by the reaction mixture at 300–380°C. All other phases are not changed in this reaction.

Table 3 presents the catalytic properties of the samples calcined in air at 400°C.

Reaction products over all the samples were pyrazinonitrile, pyrazine, and carbon oxides (CO_x). Nitrogen oxides were not found. The carbon balance in all experiments was close to 100%.

The catalysts had a stable activity starting from the first hours of service and were not deactivated under the experimental conditions.

Figure 6 presents typical plots characterizing the selectivity of reaction product formation as a function of methylpyrazine conversion (X) for the sample with Mo/P = 7.8 at 360°C. An increase in the conversion leads to a gradual decrease in the selectivity of nitrile formation and to an increase in the formation of pyrazine and carbon oxides. Note that, at a methylpyrazine conversion of 15–75%, the ratio of the selectivities to pyrazine and carbon oxides is almost constant ($S_P/S_{CO_x} \approx 4$). A detailed analysis carried out in [20] showed that this is possible if a heteroaromatic ring remains intact in the reaction, and only a substituent transforms. In this case, oxidative dealkylation occurs and one pyrazine molecule and a molecule of carbon oxide are formed from a molecule of methylpyrazine. If CO_x is formed in a larger amount than pyrazine, then one can conclude that the heterocycle participates in the reaction. This is possible at low conversions due to the destruction of methylpyrazine itself and at high conversions due to the additional oxidation of pyrazinonitrile and pyrazine.

Thus, the experimental data suggest the following scheme for the formation of products in the oxidative ammonolysis of methylpyrazine, including parallel and consecutive steps. This scheme is analogous to the scheme observed earlier in the study of the same reaction over the oxide vanadium–antimony system [20], as well as in the PMo–HPAc and PMoV–HPAc systems [10]:

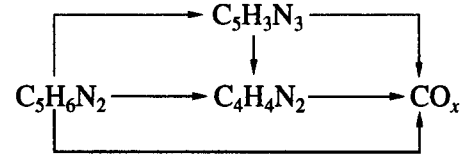

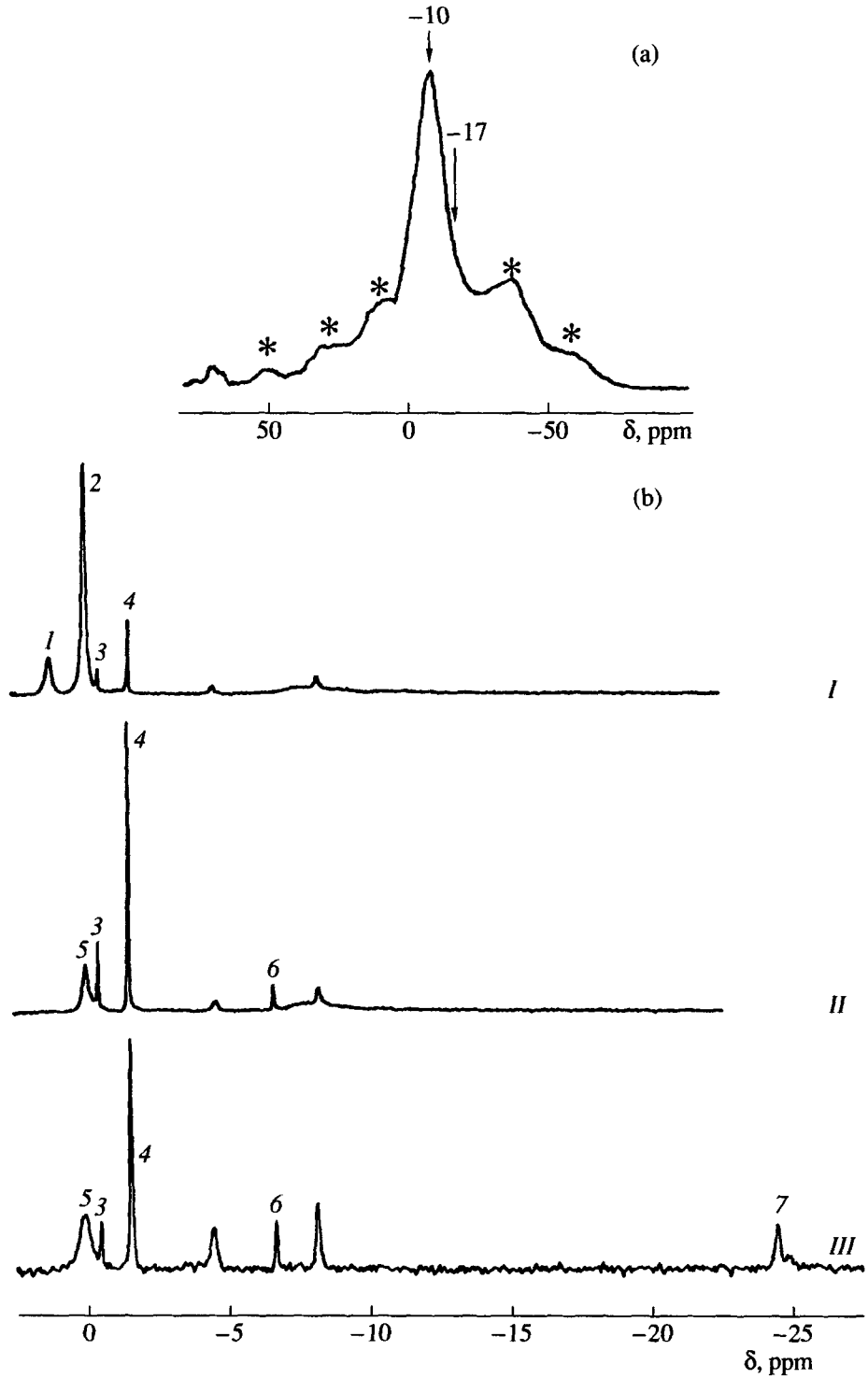

Fig. 3. ^{31}P NMR spectra of the sample with Mo/P = 7.8: (a) spectrum of a solid sample (MAS), asterisk denotes side bands due to sample rotation, (b) spectra of subsequent water extracts (*I–III*): (*1*) $[P_2Mo_5O_{23}]^{6-}$, (2) $[H_xPO_4]^{(3-x)-}$, (*3*) $[PMo_9O_{31}]^{3-}$, (*4*) $[H_yPMo_{11}O_{39}]^{(7-y)-}$, (*5*) $[PMo_{12}O_{40}]^{4-}$, (*6*) $[PMo_{12}O_{40}]^{5-}$, (*7*) $[PMo_{12}O_{38}]^{+}$. Other bands correspond to nonidentified forms, formed at the dissolution of molybdenyl pyrophosphate $(MoO_2)_2P_2O_7$.

Analysis of the data in Table 3 shows that such a scheme is common for all phosphorus–molybdenum samples; only the rates of different routes are different. For example, for the samples with Mo/P ≥ 7.8, an increase in the temperature leads to the additional oxidation of pyrazinonitrile. The lower the Mo/P ratio, the more pronounced this additional oxidation. For the samples with Mo/P ≥ 12 in the whole range of temper-

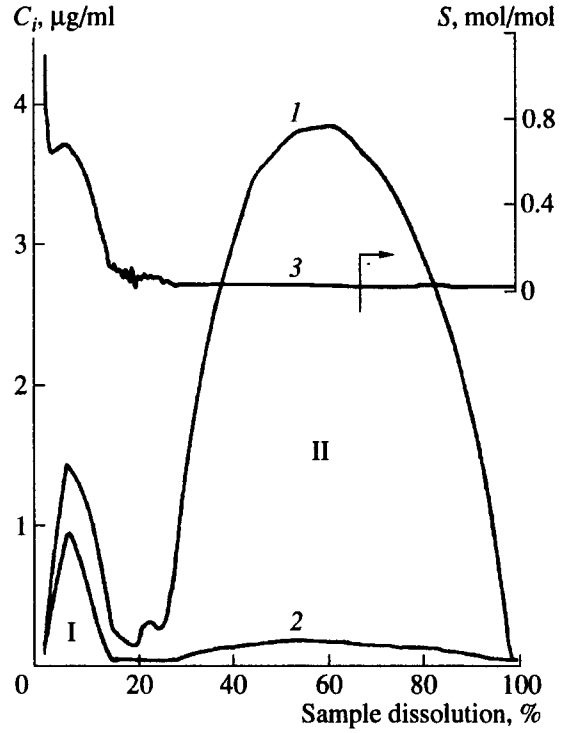

Fig. 4. (*1*) Molybdenyl and (*2*) phosphate dissolution curves and (*3*) stoichiometry curve for the sample with Mo/P = 7.8.

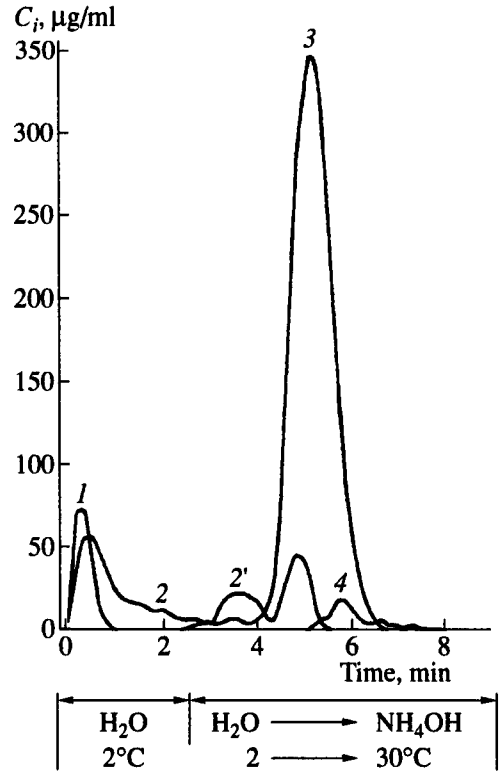

Fig. 5. Kinetic curves of phase dissolution for the sample with Mo/P = 7.8, (*1*) P_1Mo_1, (*2* and *2'*) P_1Mo_{12}, (*3*) Mo_1P_x, (*4*) Mo_1.

atures and methylpyrazine conversions, the selectivity to the product changes only slightly. That is, the contribution from the consecutive route is low. For the samples with 4.5 < Mo/P < 12, carbon oxides are largely formed via the consecutive route with the additional oxidation of nitrile and pyrazine. At Mo/P = 3 or 24.5 (particularly, in the first case), carbon oxides are formed directly from methylpyrazine via the parallel route.

It is possible to compare the catalytic properties of samples using Fig. 7, which shows the specific activity and maximal yield of pyrazinonitrile as functions of the Mo/P ratio at a reaction temperature of 360°C. An increase in the molybdenum content is accompanied by a gradual increase in the catalyst activity, particularly for the samples with Mo/P =3 and Mo/P = 4.5. The nitrile yield as a function of the system composition has a flat maximum at 68–70% corresponding to the samples with Mo/P = 7.8–12.

To reveal the active component of the phosphorus–molybdenum system, we additionally studied the catalytic properties of individual and phosphorus-modified molybdenum trioxide. The former was obtained by the thermal decomposition of ammonium paramolybdate, and the latter was obtained using the method described in [9]. Table 4 presents the activities and selectivities of the formation of reaction products over different samples at 350°C, as well as the maximal yields of pyrazinonitrile over these samples.

We see from Table 4 that individual molybdenum oxide is itself rather active and selective. Note that, in most oxidative reactions of other organic compounds, it has a very low activity. The introduction of phosphorus

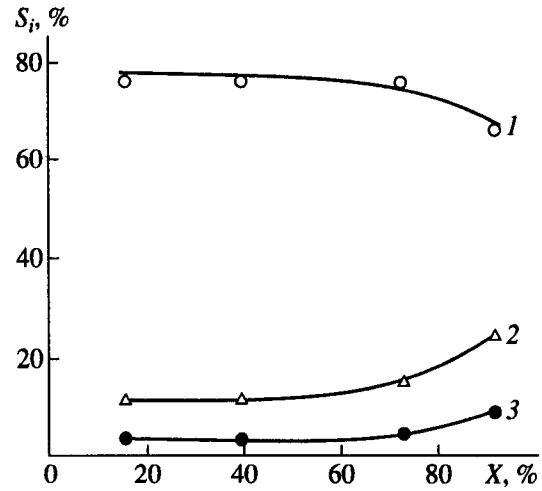

Fig. 6. Selectivity of the formation of (*1*) pyrazinonitrile, (*2*) pyrazine, and (*3*) carbon oxides as functions of methylpyrazine conversion on the sample with Mo/P = 7.8 at 360°C.

Table 3. Catalytic properties of PMo samples calcined at 400°C in the reaction of oxidative ammonolysis of methylpyrazine (the contact time is 1.8 s)

Mo/P	S_{sp}, m^2/g	Reaction temperature, °C	Conversion, %	Selectivity, %			Carbon balance, %	$C_5H_3N_3$ yield, %
				CO_x	$C_4H_4N_2$	$C_5H_3N_3$		
3	2.6	330	4.5	11.5	36.0	47.5	95.0	2.1
		340	10.0	12.5	40.2	45.5	98.2	4.6
		350	15.1	13.0	42.0	42.3	97.3	6.6
		360	22.4	16.2	54.8	24.4	95.4	5.5
		380	40.2	19.8	66.2	14.1	100.1	3.4
4.5	3.4	310	24.6	5.0	18.6	74.8	98.4	18.4
		330	68.3	5.0	20.2	69.9	95.7	47.7
		340	80.7	5.4	20.1	71.7	97.2	57.9
		350	92.4	5.6	23.2	65.0	94.1	60.1
		370	99.0	8.7	36.2	46.6	93.5	56.1
7.8	5.4	310	18.4	3.0	12.1	80.5	95.5	14.8
		330	38.0	3.1	12.8	80.0	96.0	30.4
		350	73.1	3.5	14.3	76.3	94.1	55.8
		360	92.5	4.0	16.5	74.2	94.9	68.6
		370	96.6	5.5	20.0	70.1	96.6	67.7
		380	97.6	5.0	20.8	68.4	97.2	68.7
12	4.3	300	22.5	5.4	21.5	68.8	95.7	15.5
		330	61.6	5.3	21.8	68.2	94.4	42.0
		340	81.2	5.4	22.9	67.8	95.8	55.1
		350	86.7	5.6	23.0	68.7	96.7	59.6
		360	91.5	5.4	22.6	72.9	100.4	66.7
		370	94.0	5.4	21.6	70.3	97.0	66.1
		380	96.5	5.5	22.1	72.4	100.3	69.9
24.5	5.0	320	60.1	6.6	31.2	56.1	94.9	33.7
		330	78.1	6.6	33.1	55.8	95.5	43.6
		340	90.7	6.6	32.5	55.2	96.3	50.1
		350	94.2	6.8	34.3	53.3	94.2	50.2
		360	96.8	6.7	34.1	54.9	95.7	53.1

Table 4. Comparison of catalytic properties of individual MoO_3 and binary PMo samples

Sample	Contact time, s	$k_1 \times 10^{-18}$, molecule m^{-2} s^{-1}	X, %	Selectivity of formation, %			Y_{max}, %
				CO_x	Pyrazine	Pyrazinonitrile	
MoO_3	2.5	2.2	70.0	5.3	29.3	52.4	45.0
$P_xMoO^*_{3-x}$	1.5	8.1	80.0	3.9	16.0	63.0	56.4
Mo/P = 7.8	1.5	6.6	76.8	2.7	11.9	80.6	68.7

* $x = 0.036$.

into the MoO_3 structure leads to a significant increase in both the activity and selectivity of nitrile formation. The binary sample (Mo/P = 7.8) containing additionally molybdenyl phosphates is the most selective in the formation of nitril.

Thus, the high activity and selectivity of the phosphorus–molybdenum system is due to the phases of the solid solution of phosphorus in molybdenum trioxide and of molybdenyl phosphates. The deterioration of catalytic properties of the samples with a decrease in

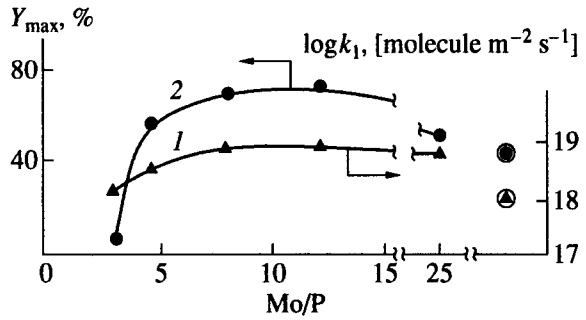

Fig. 7. (*1*) Activity of binary PMo samples and (*2*) maximal yield of pyrazinonitrile on these samples as functions of system composition. Symbols in circles present the data for individual MoO_3.

the Mo/P ratio from 4.5 to 3 seems to be due to the presence of ammonium polyphosphates in these samples.

To conclude, we note that the products of thermolysis are more active and selective in the oxidative ammonolysis of methylpyrazine, as well as in the reaction of acrolein oxidation [9], than the initial heteropoly compounds [10].

ACKNOWLEDGMENTS

The study of the phosphorus–molybdenum system by the method of differential dissolution was supported in part by the Russian Foundation for Basic Research, project no. 96-03-33087.

REFERENCES

1. FRG Patent 3 107 756, 1982.
2. US Patent 4 931 561, 1990.
3. JPN Patent 6 431 769, 1989.
4. Forni, L., *Appl. Catal.*, 1986, vol. 20, nos. 1–2, p. 219.
5. Forni, L., Oliva, C., and Rebuschini, C., *J. Chem. Soc., Faraday Trans. I*, 1988, vol. 84, no. 7, p. 2397.
6. Kagarlitskii, A.D., Krichevskii, L.A., and Suvorov, B.V., *Khim.-Farm. Zh.*, 1993, no. 3, p. 45.
7. Pope, M.T., *Heteropoly and Isopoly Oxometalates*, Berlin: Springer, 1983.
8. Kierkegaard, P., *Arkiv Kemi*, 1962, vol. 19, no. 1, p. 51.
9. Popova, G.Ya. and Andrushkevich, T.V., *Kinet. Katal.*, 1994, vol. 35, no. 1, p. 135.
10. Bondareva, V.M., Andrushkevich, T.V., Detusheva, L.G., and Litvak, G.S., *Catal. Lett.*, 1996, vol. 42, p. 113.
11. Gadzhiev, K.N., Aliev, E.A., and Khanmamedova, A.K., *Tez. dokl. V konferentsii po okislitel'nomu geterogennomu katalizu* (Proc. V Conf. on Oxidative Heterogeneous Catalysis), Baku, 1981, pt. 2, p. 58.
12. Ai, M. and Suzuki, S., *J. Catal.*, 1973, vol. 30, no. 3, p. 362.
13. Ai, M., *Kogyo Kagaku Zasshi*, 1971, vol. 74, no. 1, p. 183.
14. Ai, M. and Ishihara, M., *Kogyo Kagaku Zasshi*, 1970, vol. 73, no. 12, p. 2152.
15. Bondareva, V.M., Andrushkevich, T.V., and Plyasova, L.M., *React. Kinet. Catal. Lett.*, 1988, vol. 63, no. 1, p. 201.
16. Solov'eva, L.P., Tsybulya, S.V., and Zabolotnyi, V.A., *POLIKRISTALL—sistema programm dlya strukturnykh raschetov* (POLIKRISTALL: A Program Package of Structure Calculations), Novosibirsk: Institute of Catalysis, 1988.
17. Malakhov, V.V., Vlasov, A.A., Boldyreva, N.N., and Dovlitova, L.S., *Zavod. Lab.*, 1996, no. 2, p. 1.
18. Malakhov, V.V., *Zh. Anal. Khim.*, 1989, vol. 44, no. 7, p. 1177.
19. Maksimovskaya, R.I. and Bondareva, V.M., *Zh. Neorg. Khim.*, 1994, vol. 39, no. 8, p. 1298.
20. Bondareva, V.M., Andrushkevich, T.V., and Zenkovets, G.A., *Kinet. Katal.*, 1997, vol. 38, no. 5, p. 720.
21. Lepilina, R.G. and Smirnova, N.M., *Termogrammy neorganicheskikh fosfatnykh soedinenii* (Thermograms of Inorganic Phospate Compounds), Leningrad: Nauka, 1984.
22. Chuvaev, V.R., Mailieva, G.K., Popov, K.N., and Spitsyn, V.I., *Dokl. Akad. Nauk SSSR*, 1979, vol. 247, no. 5, p. 1165.
23. *X-ray Powder Data File ASTM, 5-0508*, Philadelphia, 1964.
24. Yurchenko, E.N., Kustova, G.N., and Batsanov, S.S., *Kolebatel'nye spektry neorganicheskikh soedinenii* (Vibrational Spectra of Inorganic Compounds), Novosibirsk: Nauka, 1981, p. 82.
25. Nakamoto, K., *Infrared and Raman Spectra of Inorganic and Coordination Compounds*, New York: Wiley, 1997.
26. Bekbutov, A.B., Il'yasova, A.K., Geskina, R.A., and Shalamov, A.E., *Izv. Akad. Nauk KazSSR, Ser. Khim.*, 1968, no. 2, p. 1.
27. Karyakin, Yu.V. and Angelov, N.N., *Chistye khimicheskie veshchestva* (Pure Chemicals), Moscow: Nauka, 1974.
28. Bondareva, V.M., Andrushkevich, T.V., Maksimovskaya, R.I., *et al.*, *Kinet. Katal.*, 1994, vol. 35, no. 1, p. 129.
29. Maksimovskaya, R.I., Bondareva, V.M., and Litvak, G.S., *Zh. Neorg. Khim.*, 1996, vol. 41, no. 7, p. 1173.
30. Maksimovskaya, R.I., *2nd Int. Memorial G.K. Boreskov Conf.*, Novosibirsk, 1997, pt. II, p. 105.